An Examination of the Threshold-Based Earthquake Early Warning Approach Using a Low-Cost Seismic Network

by Chih-Yih Hsieh, Wei-An Chao, and Yih-Min Wu

INTRODUCTION

Earthquake early warning (EEW) systems have been researched and developed in Japan, Mexico, the United States, Taiwan, and other countries (e.g., Allen *et al.*, 2009; Satriano *et al.*, 2011). One important aspect of EEW is to rapidly assess potential earthquake damage using the early portion of ongoing ground vibration. There are two types of EEW systems, namely, regional and onsite. Regional EEW systems collect and analyze seismic data from multiple stations near the epicenter and provide earthquake information (e.g., magnitude and location) to distant sites. In contrast, onsite systems use the early part of the *P* wave to predict impending ground motion for the later *S* and surface waves at the same site without necessarily estimating the source location and magnitude. Thus, onsite systems are generally faster than regional systems for near-source sites. Over the past decade, the initial peak ground displacement (P_d) and predominant period (τ_c) for the initial *P* wave have been the two most important early warning parameters used to rapidly estimate the magnitude (e.g., Wu and Kanamori, 2005a; Shieh *et al.*, 2008). Furthermore, several authors (Wu and Kanamori, 2005b; Hsiao *et al.*, 2009) have found empirical relations between the P_d and peak ground velocity (PGV) and peak ground acceleration (PGA). A threshold-based EEW approach was recently tested in several studies. For the threshold-based method, once the initial *P*-wave amplitude exceeds a certain threshold, an alarm is issued. Therefore, the EEW processing time is reduced for a faster warning. Wu and Kanamori (2005b) used 26 earthquake events ($M_w > 5.0$ and focal depth < 35 km) recorded by the Taiwan Strong Motion Instrumentation Program network. Their results indicated that $P_d > 0.5$ cm is a good indicator for the earthquake destructiveness. They also suggested the product $\tau_c \times P_d$ can improve the reliability of identifying damaging events. Based on the P_d versus PGV and τ_c versus magnitude empirical relationships, Zollo *et al.* (2010) first and Colombelli *et al.* (2012) later proposed 0.2 cm and 0.6 s as threshold values for P_d and τ_c, respectively, to identify potential damage zones (PDZs) during the occurrence of an earthquake. However, the EEW system performance can be influenced by variability in the selected time window for the initial *P*-wave data (e.g., Wurman *et al.*, 2007). This variability may also cause discrepancies when determining a threshold value for threshold-based EEW methods.

In this study, we use acceleration signals from a dense seismic network based on the microelectromechanical systems (MEMS; Holland, 2003) accelerometers built by the EEW research group at National Taiwan University (Wu *et al.*, 2013; Hsieh *et al.*, 2014; Wu, 2014). In recent years, this network has recorded numerous moderate-sized earthquakes ($5.9 \le M_L \le 6.4$). These records offer an excellent opportunity to examine the merit of different selected time windows for determining the filtered displacement threshold for faster and more robust onsite warnings.

DATA PROCESSING AND RESULTS

For this study, we analyzed 1186 real-time strong-motion records from four inland earthquakes, which were recorded by a *P*-wave alert device (*P* alert) network with epicentral distances ranging from a minimum of 2.4 km to a maximum of 218.4 km (Fig. 1). The focal depth for these events was between 14 and 20 km as reported by the Central Weather Bureau rapid reporting system. The strong ground shaking generated by these events caused landslides, rock fall, and a few casualties. Each *P*-alert station has a three-component acceleration signal with 16-bit resolution, a sampling rate of 100 Hz, and a full dynamic range of $\pm 2g$ (Wu *et al.*, 2013). We followed the data-processing procedure of Wu and Kanamori (2005a), which involved picking the first *P*-wave arrival, double integrating to obtain the displacement, and causal Butterworth filtering with a high-pass corner frequency of 0.075 Hz. The filter choice was designed to remove undesired long-period trends and baselines introduced by the double integration. The filtered vertical displacement record was then obtained, and the PGA was measured from the maximum amplitude on the unfiltered three components of accelerograms. Figure 2 shows an example of determining the PGA.

In this study, we used two early warning parameters, progressive displacement value (P_{dv}) and acceleration threshold value of 80 Gal, to rapidly issue earthquake alerts. P_{dv} is measured from the filtered vertical displacement record over a specific time window length (TWL) after the first *P* arrival time. A choice of threshold of 80 Gal is based on a previous study of Wu *et al.* (2011). They found that 76% of seismic stations exhibiting P_d values above 0.35 cm, the threshold for identifying PDZ, had PGA values larger than 80 Gal. They also suggested that a commonly adopted 3 s time window after the arrival of the *P* wave for computing warning parameters might

 doi: 10.1785/0220150073

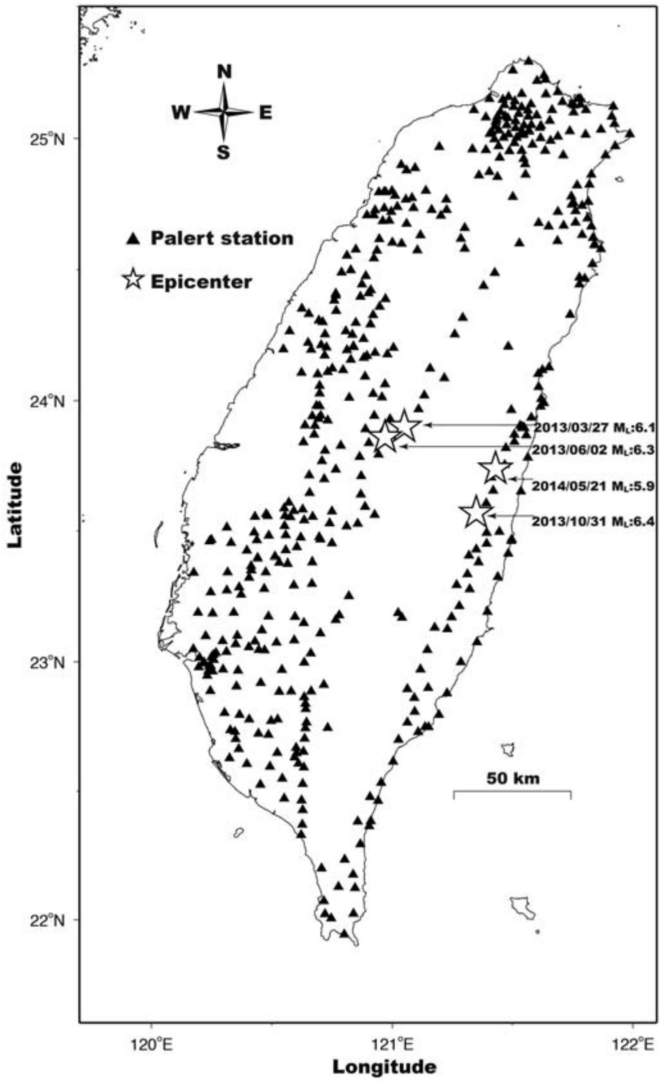

▲ **Figure 1.** Station distribution of the *P*-alert earthquake early warning system (solid triangles). The open stars indicate the earthquakes used in this study.

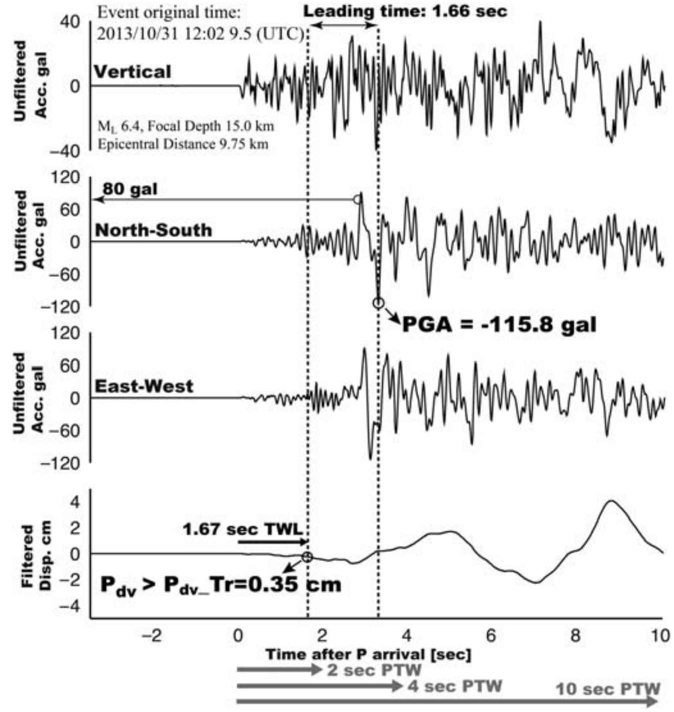

▲ **Figure 2.** Raw three-component accelerograms and 0.075 Hz high-pass filtered vertical displacement seismogram. The dashed vertical lines indicate the time points of $P_{dv} > P_{dv\_Tr} = 0.35$ cm and peak ground acceleration, respectively.

be too long for warning near-source sites. Thus, to investigate the influence of different permitted time windows (PTWs) in calculating the P_{dv} value, we used PTW values between 1 and 10 s after the first *P*-wave arrival with a 1 s increment. The threshold P_{dv} value (P_{dv_Tr}) is considered to range from 0.1 to 0.6 cm with a 0.05 cm interval. Figure 2 displays an example of determining aforementioned time window parameters of TWL and PTW. A correct alarm, missed early alarm, false alarm, and correct but no alarm are defined based on the specific P_{dv} and PGA threshold settings: (a) correct alarm, $P_{dv} > P_{dv\_Tr}$ and PGA > 80 Gal; (b) missed early alarm, $P_{dv} \leq P_{dv\_Tr}$ and PGA > 80 Gal; (c) false alarm, $P_{dv} > P_{dv\_Tr}$ and PGA < 80 Gal; and (d) correct no alarm: $P_{dv} \leq P_{dv\_Tr}$ and PGA < 80 Gal. Furthermore, the optimal performance for a threshold-based EEW method was commonly defined as a system with both higher successful detection percentage and larger leading time. Here, a successful detection includes both correct alarm and correct no alarm. The early warning leading time was defined as the time interval between when the filtered vertical displacement exceeded the P_{dv_Tr} and the time of the PGA arrival. For a station, if the time, P_{dv} exceeding the threshold value, is later than the time point with the acceleration reaching 80 Gal, the leading time was defined as the time difference between the acceleration first exceeded 80 Gal and the PGA was recorded (Fig. 2). A total of 129 acceleration records with exceeding 80 Gal are used in calculating leading times.

The resultant false alarm rates for a specific P_{dv_Tr} threshold and PTW value are summarized in Table 1. A small P_{d_Tr} and large STW yielded false alarms. For example, a $P_{dv\_Tr} < 0.35$ cm with a 3 s PTW exhibited the potential to misidentify small events as large ones, with a false alarm rate of 0.08%–2.69%. The successful detection percentage and average leading time as a function of PTW for different P_{dv_Tr} thresholds are shown in Figure 3. The successful detection rate gradually increased with increasing PTW, except for when $P_{dv\_Tr} \leq 0.2$ cm, which suddenly decayed after the PTW exceeded a specific value (e.g., 5 s PTW for $P_{dv\_Tr} = 0.1$ cm; dashed line in Fig. 3a). The average EEW leading times determined in this study are of 1.54–6.20 s (Fig. 3b) ahead of the PGA arrival. For the threshold $P_{dv\_Tr} \geq 0.25$ cm, the average leading times are less than 4 s for each PTW values (dashed line in Fig. 3b). In contrast, a high percentage (> 90%) of the successful detections with $P_{dv\_Tr} < 0.25$ cm for PTWs from 2 to 5 s exhibited larger leading times (> 4 s).

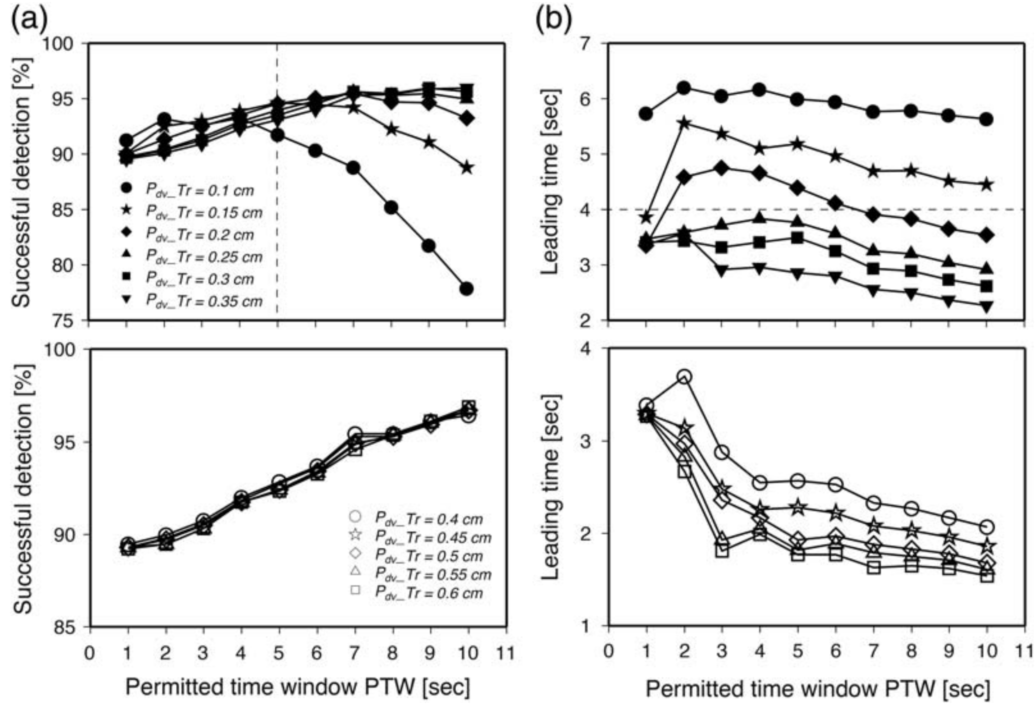

▲ **Figure 3.** (a) Rate of successful detection and (b) average leading time as function of the value permitted time window used, respectively. Different symbols correspond to different values of P_{dv_Tr}.

DISCUSSION AND CONCLUSIONS

We analyzed strong-motion records from a *P*-alert seismic network operating in Taiwan to investigate the feasibility of a threshold-based EEW approach for earthquakes with local magnitudes ranging from 5.9 to 6.4. The performance for this approach was evaluated by defining successful detection, missed and false alarms, and counting their relative percentages. A high percentage of successful detection, small number of false alarms, and sufficient EEW leading time represent the ideal results for our application. In general, a false alarm may occur with small P_{dv_Tr} and large PTW values (Table 1). In contrast, large P_{dv_Tr} and small PTW values easily missed alarms. Table 1 shows ~20% difference in the rate of false alarms between using 0.1 and 0.6 cm threshold values with a 10 s PTW. The highest successful detection appeared with 0.1 and 0.35 cm P_{dv_Tr} values for 2 and 10 s PTWs, respectively (Fig. 3a). For a specific P_{dv_Tr} threshold, we would expect that the leading times decrease with the increasing PTW value. However, leading times in some cases increase when expanding the PTW (Fig. 3b). The aforementioned phenomenon might be caused by the different data number and/or two choices of leading time in calculating average value. For real EEW applications, selecting the threshold and TWL depends on the EEW

Table 1
Rate of False Alarm with Each P_{dv_Tr} and Permitted Time Window Values

P_{dv_Tr} (cm)	1 s (%)	2 s (%)	3 s (%)	4 s (%)	5 s (%)	6 s (%)	7 s (%)	8 s (%)	9 s (%)	10 s (%)
0.1	0.08	1.09	2.69	3.87	6.06	7.83	10.02	13.97	17.68	21.80
0.15	0.00	0.08	0.76	1.35	1.94	2.61	3.54	5.89	7.66	10.19
0.2	0.00	0.00	0.17	0.51	0.76	1.18	1.68	2.69	3.54	5.30
0.25	0.00	0.00	0.08	0.25	0.51	0.76	1.18	1.77	2.44	3.45
0.3	0.00	0.00	0.08	0.17	0.34	0.59	0.93	1.35	1.77	2.69
0.35	0.00	0.00	0.00	0.08	0.25	0.51	0.76	1.09	1.60	2.36
0.4	0.00	0.00	0.00	0.08	0.25	0.42	0.51	0.93	1.26	1.68
0.45	0.00	0.00	0.00	0.00	0.08	0.34	0.42	0.76	1.09	1.43
0.5	0.00	0.00	0.00	0.00	0.08	0.34	0.34	0.59	1.01	1.26
0.55	0.00	0.00	0.00	0.00	0.08	0.34	0.34	0.51	0.93	1.26
0.6	0.00	0.00	0.00	0.00	0.08	0.34	0.34	0.42	0.84	1.01

purpose and requires different levels of uncertainty and tolerance for false or missed alarms. For example, when stopping elevators, the influence of false alarms should be small because they only take a few minutes to restart. However, having no false alarm is critical to many EEW applications where the cost for a false alarm is high, such as interrupting industrial processes. According to our results, $P_{dv\_Tr} = 0.2$ cm can be used as an early warning parameter with a 3 s PTW to provide an elevator system a 92.51% successful detection, 0.17% false alarms, and 4.75 s average leading time (Fig. 3; Table 1). In contrast, for industrial systems, the threshold $P_{dv\_Tr} = 0.35$ cm should be used to prevent false alarms (Table 1).

Our studied cases of four moderate-sized earthquakes ($5.9 \le M_L \le 6.4$) used a dense MEMS accelerometer network in Taiwan, which is desirable for threshold-based EEW implementation and providing sufficient leading time. For an acceleration threshold of 80 Gal, $P_{dv\_Tr} = 0.35$ cm, and 3 s PTW, our proposed approach provided an average 2.92 s leading time with a 90.91% successful detection rate and no false alarms, which is consistent with the off-line test results of Wu *et al.* (2011). In real applications, the progressive displacement threshold value (P_{dv_Tr}) for the onsite warning system might be modified depending on the tolerance for ground shaking and false alarm costs. We proposed a functional threshold-based EEW system relying on the filtered vertical displacement amplitude in Taiwan that could potentially save both lives and money.

ACKNOWLEDGMENTS

The authors wish to thank Simona Colombelli and an anonymous reviewer for their constructive comments that helped improve the article. This research has been supported by the Central Weather Bureau (CWB) and the Ministry of Science and Technology (MOST), Taiwan. The software package Generic Mapping Tools (Wessel and Smith, 1998) was used in this study.

REFERENCES

Allen, R. M., P. Gasparini, O. Kamigaichi, and M. Bose (2009). The status of earthquake early warning around the world: An introductory overview, *Seismol. Res. Lett.* **80,** 682–693, doi: 10.1785/gssrl.80.5.682.

Colombelli, S., O. Amoroso, A. Zollo, and H. Kanamori (2012). Test of a threshold-based earthquake early warning method using Japanese data, *Bull. Seismol. Soc. Am.* **102,** no. 3, 1266–1275, doi: 10.1785/0120110149.

Holland, A. (2003). Earthquake data recorded by the MEMS accelerometer, *Seismol. Res. Lett.* **74,** 20–26, doi: 10.1785/gssrl.74.1.20.

Hsiao, N. C., Y. M. Wu, T. C. Shin, L. Zhao, and T. L. Teng (2009). Development of earthquake early warning system in Taiwan, *Geophys. Res. Lett.* **36,** L00B02, doi: 10.1029/2008GL036596.

Hsieh, C. Y., Y. M. Wu, T. L. Chin, K. H. Kuo, D. Y. Chen, K. S. Wang, Y. T. Chan, W. Y. Chang, W. S. Li, and S. H. Ker (2014). Low cost seismic network practical applications for producing quick shaking maps in Taiwan, *Terr. Atmos. Ocean. Sci.* **25,** 617–624, doi: 10.3319/TAO.2014.03.27.01(T).

Satriano, C., Y. M. Wu, A. Zollo, and H. Kanamori (2011). Earthquake early warning: Concepts, methods and physical grounds, *Soil Dyn. Earthq. Eng.* **31,** 106–118, doi: 10.1016/j.soildyn.2010.07.007.

Shieh, J. T., Y. M. Wu, and R. M. Allen (2008). A comparison of τ_c and τ_{pmax} for magnitude estimation in earthquake early warning, *Geophys. Res. Lett.* **35,** L20301, doi: 10.1029/2008GL035611.

Wessel, P., and W. H. F. Smith (1998). New, improved version of Generic Mapping Tools released, *Eos Trans. AGU* **79,** 579.

Wu, Y. M. (2014). Progress on development of an earthquake early warning system using low cost sensors, *Pure Appl. Geophys.*, doi: 10.1007/s00024-014-0933-5.

Wu, Y. M., and H. Kanamori (2005a). Experiment on an onsite early warning method for the Taiwan early warning system, *Bull. Seismol. Soc. Am.* **95,** no. 1, 347–353, doi: 10.1785/0120040097.

Wu, Y. M., and H. Kanamori (2005b). Rapid assessment of damage potential of earthquakes in Taiwan from the beginning of *P* waves, *Bull. Seismol. Soc. Am.* **95,** no. 3, 1181–1185, doi: 10.1785/0120040193.

Wu, Y. M., D. Y. Chen, T. L. Lin, C. Y. Hsieh, T. L. Chin, W. Y. Chang, W. S. Li, and S. H. Ker (2013). A high-density seismic network for earthquake early warning in Taiwan based on low cost sensors, *Seismol. Res. Lett.* **84,** 1048–1054.

Wu, Y. M., T. L. Lin, W. A. Chao, H. H. Huang, N. C. Hsiao, and C. H. Chang (2011). Faster short-distance earthquake early warning using continued monitoring of filter vertical displacement: A case study for the 2010 Jiasian, Taiwan, earthquake, *Bull. Seismol. Soc. Am.* **101,** no. 2, 701–709.

Wurman, G., R. M. Allen, and P. Lombard (2007). Toward earthquake early warning in northern California, *J. Geophys. Res.* **112,** no. B08311, doi: 10.1029/2006JB004830.

Zollo, A., O. Amoroso, M. Lancieri, Y. M. Wu, and H. Kanamori (2010). A threshold-based earthquake early warning using dense accelerometer networks, *Geophys. J. Int.* **183,** 963–974, doi: 10.1111/j.1365-246X.2010.04765.x.

Chih-Yih Hsieh
Wei-An Chao
Yih-Min Wu[1]
Department of Geosciences
National Taiwan University
1 Roosevelt Road Sec. 4
Taipei 10617, Taiwan
vvnchao@gmail.com

Published Online 16 September 2015

[1] Also at National Center for Research on Earthquake Engineering, National Applied Research Laboratories, Taipei, Taiwan.